HHS Public Access

Author manuscript

Neuron. Author manuscript; available in PMC 2017 September 07.

Published in final edited form as:

Neuron. 2016 September 7; 91(5): 1085–1096. doi:10.1016/j.neuron.2016.07.044.

Coupled activation of primary sensory neurons contributes to chronic pain

Yu Shin Kim[1,2,*,†], **Michael Anderson**[1,†], **Kyoungsook Park**[1,†], **Qin Zheng**[1,†], **Amit Agarwal**[1], **Catherine Gong**[1], **Saijilafu**[3,4], **LeAnne Young**[1], **Shaoqiu He**[6], **Pamela Colleen LaVinka**[1], **Fengquan Zhou**[3], **Dwight Bergles**[1], **Menachem Hanani**[5], **Yun Guan**[6], **David C. Spray**[7], and **Xinzhong Dong**[1,8,*]

[1]Departments of Neuroscience, Neurosurgery, Dermatology, Center of Sensory Biology, the Johns Hopkins University School of Medicine, 725 N. Wolfe Street, Baltimore, MD 21205 USA

[2]Department of Neuroscience & Cell Biology, the University of Texas Medical Branch School of Medicine, 301 University Boulevard, Galveston, TX 77555 USA

[3]Department of Orthopaedic Surgery, the Johns Hopkins University School of Medicine, 725 N. Wolfe Street, Baltimore, MD 21205 USA

[4]Department of Orthopaedics, the First Affiliated Hospital, Orthopaedic Institute, Soochow University, P.R. China

[5]Hadassah-Hebrew University Medical Center, Mt. Scopus, Jerusalem, 91240 Israel

[6]Department of Anesthesiology, the Johns Hopkins University School of Medicine, 725 N. Wolfe Street, Baltimore, MD 21205 USA

[7]The Dominick P. Purpura Department of Neuroscience, Albert Einstein College of Medicine, Bronx, New York 10461

[8]Howard Hughes Medical Institute, the Johns Hopkins University School of Medicine, Baltimore, MD 21205, USA

SUMMARY

[*]Co-correspondence: Xinzhong Dong, The Solomon H. Snyder Department of Neuroscience, Johns Hopkins University School of Medicine, 725 N. Wolfe Street, Baltimore, MD 21205, Phone: 410-502-2993, Fax: 410-614-6249, xdong2@jhmi.edu. Yu Shin Kim, Department of Neuroscience & Cell Biology, University of Texas Medical Branch, 301 University Blvd., Galveston, TX 77555, Phone: 409-772-5481, Fax: 409-762-9382, yukim@utmb.edu.

[†]These authors contributed equally to this work.

Author contributions Y.S.K. conceived the project, designed and performed most imaging and behavioral experiments and wrote and edited the paper. Y.S.K. and K.P. analyzed the data. K.P. and Q.Z. performed *in vivo* DRG surgery and imaging and behavioral experiments. S. performed *in vivo* DRG surgery with supervision from F.Z. C.G. and S.H. performed immunohistochemistry with supervision from Y.G. C.G. and L.Y. counted cell size and number. Y.S.K., K.P., C.G., and L.Y. maintained, setup mating, took care of mice and performed genotyping. D.C.S. performed the patch clamp recordings. A.A. and D.B. generated Rosa26-LSL-GCaMP6s mice. P.C.L. and M.H. wrote and edited the paper. X.D. supervised the project and wrote and edited the paper.

The authors declare no competing financial interests.

Primary sensory neurons in the DRG play an essential role in initiating pain by detecting painful stimuli in the periphery. Tissue injury can sensitize DRG neurons, causing heightened pain sensitivity, often leading to chronic pain. Despite the functional importance, how DRG neurons function at a population level is unclear due to the lack of suitable tools. Here we developed an imaging technique that allowed us to simultaneously monitor the activities of >1,600 neurons/DRG in live mice and discovered a striking neuronal coupling phenomenon that adjacent neurons tend to activate together following tissue injury. This coupled activation occurs among various neurons and is mediated by an injury-induced upregulation of gap junctions in glial cells surrounding DRG neurons. Blocking gap junctions attenuated neuronal coupling and mechanical hyperalgesia. Therefore, neuronal coupling represents a new form of neuronal plasticity in the DRG and contributes to pain hypersensitivity by "hijacking" neighboring neurons through gap junctions.

INTRODUCTION

Dorsal root ganglion (DRG) are aggregates of the somata of 10,000–15,000 primary sensory neurons (Schmalbruch, 1987; Sorensen et al., 2003), which play an essential role in initiating somatosensation by detecting sensory stimuli in the periphery and sending signals to the spinal cord via their axons (Basbaum et al., 2009). DRG neurons are highly diverse in terms of cell sizes, gene expression, myelination levels, etc. While small-diameter neurons are the pain-sensing neurons, medium-to-large diameter neurons preferentially detect low threshold non-painful mechanical stimulation (Basbaum and Woolf, 1999; Liu and Ma, 2011). Pathological conditions such as inflammation and nerve injury can sensitize DRG neurons, causing heightened pain sensitivity, often leading to chronic pain. In addition, each DRG neuronal soma is surrounded by multiple satellite glial cells (SGCs) (Hanani, 2005; Pannese, 2010). There is evidence for intercellular communications within sensory ganglia, involving both neurons and SGCs (Hanani, 2012; Huang et al., 2013). This communication can be altered by injury. Although the mechanisms of hypersensitivity of individual neurons have been extensively studied, how DRG neurons function at a population level as an ensemble under physiological and pathological conditions is unclear due to the lack of suitable tools.

In this report, we developed an imaging technique that allowed us to simultaneously monitor the activation of >1,600 neurons/DRG in response to mechanical stimulation applied to the skin in live mice. Using this powerful technique we discovered a striking neuronal coupling phenomenon that adjacent neurons tend to activate together following inflammation or nerve injury, although this rarely happens in naïve animals. This coupled activation occurs among various sizes of neurons including small-diameter nociceptors and large-diameter low-threshold mechanoreceptors. The transfer of membrane impermeable dye between coupled-activating neurons suggests that the coupled activation is likely due to direct cell-to-cell communication. Combining the imaging technique with pharmacological and genetic approaches, we found that the coupling is mediated by an injury-induced upregulation of gap junctions in SGCs surrounding DRG neurons. Blocking gap junctions significantly attenuated neuronal coupling in the DRG and also reduced mechanical hyperalgesia. Therefore, neuronal coupling represents a new form of neuronal plasticity in the DRG and

by “hijacking” neighboring neurons through gap junctions it contributes to pain hypersensitivity.

RESULTS

Development of in vivo DRG imaging technique

In order to monitor the activity of large populations of DRG neurons in intact live animals, we developed an *in vivo* imaging technique using Pirt-GCaMP3 mice, in which the genetic-encoded Ca^{2+} indicator GCaMP3 is specifically expressed in >95% of all DRG neurons under the control of the Pirt promoter (Kim et al., 2014). For the *in vivo* imaging from anesthetized Pirt-GCaMP3 mouse, we first surgically exposed the dorsal aspect of the right lumbar 4 (L4) DRG, which innervates the right hindpaw, leg, thigh, and back of the mouse. Then the animal was laid on its abdomen on the stage under a Leica LSI confocal microscope with a long-working distance lens (Figure 1A). The spinal column was clamped to minimize movements from breathing and heart beats. During the imaging session, which usually lasted 3–4 hrs, the animal was under constant isoflurane anesthesia and its body temperature was kept at 37 °C with a heat pad. Because the surface of DRG is curved, z-stack imaging is required to cover the entire area of exposed L4 DRG. Strikingly, an average of 1,607±27 neurons per DRG (~15% of total DRG neurons) could be imaged at ~6.35 s/frame (Figure 2A and Figure 1B). To determine how well the imaged neurons represent the whole population of the ganglion, we injected the neuronal tracer DiI into the hindpaws and found that the DiI-labeled somata were evenly distributed in the DRG (Figure 1C,D). These data suggest that somata that send axons to the hindpaw are not clustered in a particular region of the DRG and the 1,600 neurons imaged are representative of the entire neuronal population. To determine the extent of DRG neurons responding to sensory stimuli in the receptive field, we performed hindpaw DiI retrograde tracing combined with GCaMP imaging experiments using naïve Pirt-GCaMP3 mice (Figure 1E,F). We stimulated the hindpaw with either mechanical force (see details in the next section) or chemicals. We found that 26.4% and 27.6% of DiI labeled neurons responded to the press of the hindpaws and the capsaicin injection into the hindpaw, respectively, and 3.4% of Dil labeled neurons responded to both stimuli. The rest of Dil labeled neurons did not respond to either stimulus. These data indicate that GCaMP3 imaging under isoflurane anesthesia allowed us to image a large portion (>50%) of neurons that innervate the receptive field. Furthermore, using a different anesthesia (i.e. pentobarbital), a similar number of neurons are activated by the same pressure (Figure 1I).

To test the specificity of neuronal activation monitored by GCaMP3 in vivo imaging, we generated *Pirt-GCaMP3;TRPV1*$^{-/-}$ mice and *Pirt-GCaMP3;TRPA1*$^{-/-}$ mice (Figure 1G,H). As expected, the injection of capsaicin or mustard oil into the hindpaws evoked robust neuronal activation in the L4 DRG of Pirt-GCaMP3 WT mice, whereas few GCaMP3 signals were detected in *Pirt-GCaMP3;TRPV1*$^{-/-}$ mice or *Pirt-GCaMP3;TRPA1*$^{-/-}$ mice, respectively. These data suggest that GCaMP signals detected during in vivo DRG imaging are ligand/channel specific.

Increased activation of small-diameter neurons contributes to mechanical hyperalgesia

For mechanical force evoked intracellular Ca^{2+} transient in neurons, we used a Rodent Pincher Analgesia Meter instead of von Frey filaments, which allowed us to accurately apply and monitor mechanical force to a large area of the hindpaws. We first determined the force needed to evoke pain responses using the device. Because of the large contact surface area of the pincher, the paw withdrawal threshold (PWT) in naïve mice is close to 500 g (Figure 2B), which is much higher than the force normally applied with the thinner von Frey filaments, however the pressure is similar. The PWTs were substantially lower (~250 g) in mice with inflammation in the hindpaw caused by complete Freund Adjuvant (CFA) injection or chronic constriction injury (CCI) of sciatic nerves (Figure 2B). Therefore, mechanical hyperalgesia and allodynia under inflammatory and nerve injury conditions were reliably evoked and accurately measured by the device. To activate neurons during the imaging experiments, we applied 250–300 g force onto the hindpaw, a force that was not enough to induce a paw withdrawal response in naïve mice, but well above the PWT after injury. The basal GCaMP3 green fluorescence level was low in the DRG (Figure 2C,E, left panels). Hindpaw stimulation evoked robust and transient Ca^{2+} increases in a few neurons in naïve mice, on average 12.7±3.0 per DRG (Figure 2C,E, right panels and Figure 2D,F and Movie S1). However, the number of activated neurons was more than doubled to 42.8±4.5 and 32.3±6.3 in the DRGs of CFA and CCI-treated mice, respectively (Figure 2G and Movie S2). The average Ca^{2+} transients in activated neurons from injured animals were significantly higher than those from naïve animals (Figure 2D,F). The diameters of the somata of activated neurons in the injured animals were significantly smaller than those in naïve mice (23.0±1.2 μm for control versus 20.2±0.4 μm for CFA and 19.9±0.4 μm for CCI) (Figure 4A). The proportion of the neurons activated by pressure that were in the small diameter (20 μm) category was also significantly higher in CFA treated mice compared with controls (52.5±4.4% for CFA vs 28.9±2.6% for control; Figure 2H). These data correlate well with the results from behavioral tests, suggesting that the increased activation of small-diameter neurons (presumably nociceptors) contributes to mechanical hyperalgesia.

Neuronal coupling occurs after tissue injury

We noticed a striking pattern of neuronal activation in the DRG of injured mice: many activated neurons (13.1±1.7 and 9.8±2.6 neurons/imaged DRG for CFA and CCI, respectively) were adjacent to each other and formed clusters of 2–5 cells, a phenomenon we called ‘coupled activation’ (Figure 3A,B and Movie S3). Neuronal coupling was defined as two or more neuronal cell bodies located within 1 μm of each other showing increases in GCaMP signals between two imaging frames (0.47 sec/frame; see faster scanning below). Importantly, coupled activation was rarely seen in naïve animals (1.3±0.5 neurons/DRG). In CFA injected mice, 29.0±1.8% of total activated neurons were coupled activated compared with 5.0±1.7% in DRG from naïve mice (Figure 3C). Similar results were obtained for the CCI mice (29.2±8.4% of total activated neurons versus 6.4±1.6% for sham operated mice). In addition, we performed in vivo DRG imaging 7 days after CFA injection as the animal is recovering from peak inflammation and found that 12.9±0.7% of total activated neurons are coupled which is significantly lower than that of 2 days post CFA (29.0%).

We then imaged the entire DRG to identify coupled activated neurons and verified coupling events using a much higher scanning speed by zooming in on one ensemble of neurons. For this experiment we used Pirt-GCaMP6 mice which we recently generated by crossing Pirt-Cre and Rosa26-loxP-STOP-loxP-GCaMP6s mice. Indeed, even with much faster imaging speed (0.47 sec/frame), we could still detect the simultaneous activation in the majority of the coupled neurons (9 out of 12 neurons exhibiting simultaneous activation; Figure 4D).

In addition to investigating a single mechanical force (i.e. ~250g) evoked response, we performed the full dose response of pressure (from very mild 50g to noxious 500g) using Pirt-GCaMP6 mice (Figure 4E-G). From mild pressure (150g and 200g) to noxious pressure (500g), there are significantly more neurons being activated in naïve mice. However, neither the number of coupled activated neurons nor the percentage of coupled neurons over total activated neurons in naïve mice are significantly increased between innocuous and noxious pressure. Strikingly, in the CFA treated mice, both the total number of coupled activated neurons and the percentage of coupled neurons over total activated neurons are significantly increased from mild pressure to noxious pressure and significantly higher than those of naïve mice. Together these data suggest that neuronal coupling is caused by tissue injury.

Although the majority of the coupled activation (75%) occurred simultaneously (i.e. no delayed activation in the coupled neurons at 0.47 sec/frame rate) and many different diameter neurons were involved in coupling events (Figure 3D and Figure 4B,C), there were a few coupling events where neurons had delayed longer than 1 sec after the first event. The delayed coupled activations were useful for determining which type of following neurons were recruited by which type of leading neurons after injury. To determine whether large-diameter low threshold mechanoreceptors (LTMR) participate in coupling activation, we generated NPY2r-tdTomato; Pirt-GCaMP3/+ mice. A previous study has shown that NPY-2r is specifically expressed in rapidly adapting Aβ-LTMRs having medium to large diameters (20–30 μm) (Li et al., 2011). We found that some of coupled activating neurons displayed red fluorescent in NPY2r-tdTomato;Pirt-GCaMP3/+ mice treated with CFA, indicating that rapid adapting Aβ-LMTRs are involved (Figure 3E). In addition, we used capsaicin to probe TRPV1-expressing neurons and found that 12.9% of capsaicin sensitive neurons are coupled activated neurons. Besides studying mechanical force-evoked neuronal coupling, we performed in vivo DRG imaging in response to noxious heat stimuli using CFA treated Pirt-GCaMP3 mice (Figure 4H,I). With hindpaw immersion into 48 °C water bath, a tot al of 110 neurons are activated, 14% of which are coupled activated neurons. Interestingly, this 14% coupling rate evoked by noxious heat is significantly lower than that induced by mechanical stimuli (>25%).

Gap-junctions likely connect coupled-activated neurons

Since DRG from both CCI− and CFA-treated mice displayed similar degrees of coupled activation, we focused on the simpler CFA model for the subsequent studies. Previous studies have demonstrated that injury induces an increase in dye transfer among glia and between neurons in the DRG implying the formation of gap junctions in the DRG after injury (Blum et al., 2014; Dublin and Hanani, 2007; Huang et al., 2010). However, how gap junctions influence neuronal activation is unclear. To test the hypothesis that gap junctions

are involved in the coupled activation, we injected rhodamine, a low molecular weight red dye which crosses gap junctions, into one of the coupled-activated neurons. Strikingly, the red fluorescence appeared in the adjacent co-activated neurons within a few min after the injection (Figure 3F). The dye-transfer occurred in 4.4% of injected coupled-activated neurons, whereas we have never seen any dye transfer from singly activated neurons. These data strongly suggest that coupled activation is mediated by cell-to-cell communication, and gap junctions are good candidates. The 4.4% rate of dye transfer is consistent with the reported low incidence of neuron-neuron dye-coupling after CFA injection in the mouse paw and also in rats after sciatic nerve ligation (Dublin and Hanani, 2007; Zuriel and Devor, 2001). Since SGCs are extremely small and tightly ensheathe neurons, it is impossible to observe them with our imaging system. Instead, we performed glia-neuron dye injection experiment on cultured DRG. SGCs have clear morphological differences and can be easily distinguished from Schwann cell-like glia (see details in our previous study: (Belzer et al., 2010)). In fact, the vast majority of glia in DRG cultures are SGCs. Indeed, we found that 10% of injected glia exhibited dye transfer to neighboring neurons (Figure 3G). Based on subsequent pharmacological and genetic data we conclude that monitoring dye transfer is not a sensitive way to determine gap junctions between neurons (directly or indirectly through SGCs). A more sensitive method to detect cell coupling is by patch clamp recordings from neuron-SGC pairs in dissociated DRG. Recordings SCG-neuron pairs, showed that 7 of 14 pairs were coupled (with junctional conductances of 8.8±2.6 nS). In all three pairs tested, 2 mM heptanol (a gap junction blocker) uncoupled cells, consistent with gap-junction mediated coupling (Figure 3H). Similar results were obtained from recording SCG-neurons pairs of acutely dissociated DRG from CFA-treated mice with junctional conductances of 5.6±2.4 nS (7 of 12 pairs; Figure S1). Furthermore, dual patch recordings of neuron-neuron pairs in acutely dissociated DRG from CFA-treated mice showed that electrical coupling occurred in 8 of 18 pairs with the junctional conductance of 0.16±0.07 nS. The junctional conductance suggest that neuron-neuron coupling is weaker that neuron-SGC coupling. Thus, it is conceivable that the observed neuronal coupling is due to neuron-SGC-neuron coupling (see discussion below).

Blockade of gap junctions reduces neuronal coupling and mechanical hyperalgesia

We next examined whether the gap junction blocker, carbenoxolone (CBX) (Zhang et al., 2009), can inhibit coupled activation. After the first imaging session which showed that 31.9±3.0% of total activated neurons in CFA treated mice are activated in clusters, we applied CBX systemically into the mice by i.p. injection (100 mg/kg) (Figure 5A–C). We performed the second imaging session 1 h later and found that only 12.5±3.0% of total activated neurons were coupled activated (Figure 5A–C and comparing Movie S4 for after CBX treatment with Movie S3 for before CBX treatment, respectively). As a control, we injected vehicle in CFA treated animals and found that it did not significantly reduce the percentage of coupled activation (before 33.5±4.2% versus after 29.1±5.6%; p=0.51; Figure 5C). This result rules out the possibility that the decreased coupling seen in CBX treatment is due to the desensitization from the multiple imaging sessions and mechanical stimulations. Systemic treatment with heptanol, a different gap junction blocker, also significantly blocked neuronal coupling in CFA treated mice (25.4±3.8% vs 10.8±2.7% of total activated neurons are coupled for pre- and post (30 min)-injection of heptanol

(0.1mg/kg in 0.9% saline; i.p.; n=3 per group; p=0.01). To minimize indirect actions of CBX, we injected it locally near the coupled activated neurons in the DRG. The results obtained with this local treatment were similar to those observed with systemic CBX (Figure 5D,E and Movies S5,6). Finally, CBX-treated mice exhibited less mechanical hyperalgesia in CFA and CCI pain models than control vehicle treated mice (Figure 5F).

Several subtypes of connexin (Cx) proteins, the components of gap junctions, including Cx37, 43, 46 have been implicated in chronic pain by previous studies (Garrett and Durham, 2008; Ohara et al., 2008). We were able to detect only Cx43 staining in the DRG, which was restricted to SGCs. The level of Cx43 protein significantly increased in the DRG after injury but not in the spinal cord (Figure 6A–D and Figure S2). To directly test whether Cx43 is required for coupled activation, we generated a DRG specific deletion of Cx43 mice (*PLP-CreER;Cx43*$^{fl/fl}$) from crossing Cx43$^{fl/fl}$ mice with proteolipid protein (PLP)-CreER mice, which is present in glial cells in the peripheral nervous system such as SGCs (Doerflinger et al., 2003). Anti-Cx43 antibody staining demonstrated that PLP-driven CreER specifically deleted Cx43 expression in SGCs in the DRG (Figure S2A,B), but it was still present in the spinal cord (likely in astrocytes) (Figure S2C,D). Therefore, *PLP-CreER;Cx43*$^{fl/fl}$ mice (Cx43CKO) allowed us to examine the function of Cx43 in SGCs. *In vivo* DRG imaging of *PLP-CreER;Cx43*$^{fl/fl}$;Pirt-GCaMP3/+ and control litter mates, which do not express Cre, showed that deletion of Cx43 in the DRG significantly attenuated the incidence of coupled activation after CFA treatment compared with litter mate controls (Figure 6E,F). Consistent with this, *PLP-CreER;Cx43*$^{fl/fl}$ mice exhibited less mechanical hyperalgesia than littermates following CFA injection (Figure 6G). However, the mutant mice have normal baseline pain sensitivity as well as normal thermal hyperalgesia after CFA treatment (Figure S1; see discussion below).

DISCUSSION

Pain manifests itself in a wide range of disorders that debilitate billions of people worldwide, causing heavy societal and health burdens. It is known that DRG neurons are responsible for the detection of noxious stimuli, and their plasticity contributes to persistent pain. However, how DRG neurons function under physiological and pathological conditions are poorly understood due to the lack of suitable tools. Because DRGs are deeply embedded in the vertebrae, it is difficult to record neuronal activity electrophysiologically *in situ*. Most of the available information is from studies on cultured or isolated ganglia, where the activity of single neurons was recorded. Currently, recording of single DRG neurons in live animals can only be achieved in few laboratories (Ma et al., 2010). The new *in vivo* DRG imaging method using the genetically-encoded Ca^{2+} indicator GCaMP that we have developed allowed us to observe cellular interactions under conditions that are close to physiological and enabled the correlation between coupled activation of neurons and pain behavior. Neuronal coupling represents a novel form of neuronal plasticity that is difficult to detect by conventional single neuron recordings. Therefore, *in vivo* DRG imaging will open new avenues to study the role of primary sensory neurons in different somatosensations including pain, itch, and touch.

Neuronal ‘cross talk’ has been first described by Devor and Wall (Devor and Wall, 1990), and was proposed to be mediated chemically (Amir and Devor, 1996). Here our dual patch recordings provided direct evidence for both neuron-SCG and neuron-neuron electrical coupling. To our best knowledge this is the first direct demonstration of such coupling. We also show that DRG neurons communicate at least in part by gap junctions. However, our results do not exclude chemical communications as proposed by previous studies. The patch clamp recordings, dye coupling, and Cx43CKO results suggest that SGCs participate in coupled activation. Indeed the major mechanism by which astrocytes communicate is by calcium waves, which are mediated via both gap junctions and chemical messengers (Scemes and Giaume, 2006). This also appears to hold for sensory ganglia, where both neurons and SGCs participate in these waves (Suadicani et al., 2010). The pathway connecting the neurons is not clear, but transmission from neuron-to-SGC-to-neuron is feasible, with neurons and SGCs forming heterotypic gap junctions (i.e. Cx43 hemichannels in glia connect with other connexin hemichannels in neurons) (Damodaram et al., 2009), (Thalakoti et al., 2007). A scheme where SGCs intervene chemically between neurons has been proposed (Rozanski et al., 2013). Both our imaging (Figure 4H,I) and behavioral data (Figure S1) suggest that neuronal coupling induced by tissue injury contributes more to mechanical hyperalgesia and allodynia than heat hyperalgesia, which requires further investigation. Coupled neuronal activation represents a novel mechanism underlying mechanical hyperalgesia (stronger pain by recruiting more nociceptors) and allodynia (non-painful LTMRs recruiting nociceptors). Therefore inhibiting gap junction-mediated coupling may provide a novel way to relieve mechanical hyperalgesia and allodynia.

METHODS

Animals

Pirt-GCaMP3 mice were generated and described in a previous study (Kim et al., 2014). Briefly, the animal is generated by targeted homologous recombination to replace the entire coding region of the Pirt gene with the GCaMP3 sequence and put in frame with the Pirt promoter. GCaMP3 cDNA was provided by the laboratory of Loren Looger (Janelia Research Campus, VA, U.S.A.). Conditional Cx43KO mice were made by crossing between loxp-ROSA-Cx43 mice and PLP-CreERT mice which were obtained from Jackson Lab (Bar harbor, ME, U.S.A). Npy2r mice were obtained from Gensat. Pirt-GCaMP6s mice were generated by crossing Pirt-Cre with Rosa26-LoxP-STOP-LoxP-GCaMP6s mice. *Pirt-GCaMP3* and Pirt-GCaMP6s heterozygotes were used in all animal experiments otherwise indicated.

Animal models

All experiments were performed in accordance with a protocol approved by the Animal Care and Use Committee at the Johns Hopkins University School of Medicine. Animals were group-housed, unless otherwise mentioned, at 23°C with ad libitum access to food and water in a regular light/dark cycle. The mice used in the tests were backcrossed to C57Bl/6 mice for at least ten generations and were 3 to 4 month-old (20–30 g) from both sexes genders. To generate the CFA inflammatory model, CFA and saline were mixed 1:1 ratio and injected

(10 μl) subcutaneously into glabrous skin of the hindpaw. Two days later imaging experiments and/or behavioral experiments, and immunohistochemistry were performed.

To generate the sciatic nerve (SN)-CCI nerve injury model, mice were anesthetized with sodium pentobarbital (40–50 mg/kg, i.p.). SN was exposed at the level of the mid-thigh by a small dissection and the nerve was isolated from surrounding tissues. The chronic constriction injury was performed by wrapping loose nylon ligatures around the unilateral SN. The incision was closed with sutures or tissue glue. Sham-operated mice received only an identical dissection of the unilateral nerve exposure and nerve isolation without the ligature. Seven to ten days after the SN-CCI surgery, imaging and behavioral experiments, and immunohistochemistry were performed.

Tamoxifen injection

Ten mg of tamoxifen (Sigma) were dissolved in 1 ml of 100% sunflower oil and made freshly before use. Cx43 WT and Cx43CKO mice both received tamoxifen injection (by gavage) at 100 mg/kg once before (usually 7 days before) the experiment was performed. Cx43CKO refers to mice that received tamoxifen injection. Behavioral assays were performed on mice after 7 days of tamoxifen injection. Cx43CKO mice were healthy and there was no visible difference compared to Cx43 WT littermate control mice, in which only PLP-CreERT gene was missing.

Behavioral tests

Behavioral tests were conducted by experimenters blind to conditions. To test paw withdrawal threshold (PWT), mice were placed in a 2.5 cm diameter tube and habituated to the tube in a behavioral room for at least 30 min per day for 3 days prior to any testing procedures. The hindpaws were outside the tube enabling mechanical stimulation. Rodent pincher analgesia meter (IITC Life Science Inc., CN, product #2450) was pressed to the hindpaws and an active withdrawal of the stimulated hindpaw or any vocalization during the press was defined as a response. The pincher meter was applied 10 times at intervals of at least 30 sec.

Hot plate methods—Mice were placed in a clear plexiglass cylinder on top of a temperature-controlled metal plate (Life Science Series 8, Model 39.) The latency of acute nocifensive responses was determined by the onset of hindpaw lifts and/or licking, flinching, or jumping.

Tail immersion test—Mice were restrained in an apparatus made of 50 mL conical tubes. Their tails were exposed in the water bath set to the designated temperatures.

Von Frey methods—Mice were placed in a transparent plastic box (4.5 × 5 × 10 cm) on a metal mesh and acclimatized for 30 minutes prior to testing. Each mouse was tested more than 5 times at a specific force manually, and the threshold was determined by the lowest force needed to elicit responses more than 50% of the time.

Hargreaves test—Mice were placed under a transparent plastic box (4.5 × 5 × 10 cm) on a glass platform (Plantar Test Apparatus, IITC Life Science). Radiant heat was adjusted to 18% of maximal output and shone on the center of the paws. Each mouse was tested more than 3 times, with each test performed 20 minutes apart.

DRG exposure surgery for *in vivo* imaging of the whole L4 DRG

For all imaging experiments, mice three months or older were anesthetized by i.p. injection of sodium pentobarbital (40–50 mg/kg, i.p.). After deep anesthesia was reached, the animal's back was shaved and aseptically prepared, and ophthalmic ointment (Lacrilube; Allergen Pharmaceuticals, Irvine, CA) was applied to the eyes to prevent drying. During the surgery, mice were kept on a heating pad (DC temperature controller, FHC) to maintain body temperature at 37 ± 0.5°C as monitored by a rectal probe.

Dorsal laminectomy in DRG was performed usually at spinal level L6 to S1 below the lumbar enlargement (but occasionally at lower than S1) but without removing the dura (some experimental conditions such as direct local drug injection into DRG tissue and rhodamine injection into DRG neurons required the removal of the dura). A 2 cm long midline incision was made around the lower part of the lumbar enlargement area; next, 0.1 ml of 1% lidocaine was injected into the paravertebral muscles and these were dissected away to expose the lower lumbar part which surrounds (L3–L5) vertebra bones. The L4 DRG transverse processes were exposed and cleaned. Using small rongeurs, the surface aspect of the L4 DRG transverse process near the vertebra was removed (only the L4 DRG transverse process was removed but the bone over the spinal cord was intact) to expose the underlying DRG without damaging the DRG and spinal cord. Bleeding from the bone was stopped using styptic cotton.

In vivo DRG calcium imaging

In vivo imaging of whole L4 DRG in live mice was performed for 1–6 hrs immediately after the surgery. Body temperature was maintained at 37 ± 0.5°C on a heating pad and rectal temperature was monitored. After surgery mice were laid down in the abdomen down position on a custom designed microscope stage. The spinal column was stabilized using custom designed clamps to minimize movements caused by breathing and heart beats. In addition, a custom designed head holder was also used as an anesthesia/gas mask. The animals were maintained under continuous anesthesia for the duration of the imaging experiment with 1–2% isoflurane gas using a gas vaporizer. Pure oxygen air was used to deliver the gas to the animal.

The microscope stage was fixed under a laser-scanning confocal microscope (Leica LSI microscope system), which was equipped with macro based large objective and fast EM-CCD camera. Live images were acquired at typically 8–10 frames with 600 Hz in frame-scan mode per 6–7 s, at depths below the dura ranging from 0 to 70 μm, using an 5X 0.5 N.A. macro dry objective, at typically 512X512 pixel resolution with solid diode lasers (Leica) tuned at 488 and at 532 nm wavelength, and emission at 500–550 nm for green and 550–650 nm for red fluorescence, respectively. For analysis, raw image stacks (512X512 to 1024X1024 pixels in the *x–y* plane and 20–30 μm voxel depth; typically 10 optical sections)

were imported into Image J (NIH) for further analysis. DRG neurons were at the focal plane and imaging was monitored during the activation of DRG neuron cell bodies by peripheral stimuli. Red fluorescent signal was used to identify Npy2r cell type, DiI tracing and rhodamine transfer. The imaging parameters were chosen to allow repeated imaging of the same cell over many stimuli, without causing damage to the imaged cells or to surrounding tissue.

Stimulus delivery during imaging experiments

Press stimuli were delivered using rodent pincher analgesia meter, which was pressed to the hindpaws of mice. The press force was controlled manually by the experimenter. The duration of the press is 15–30 sec after 40 to 50 sec of baseline imaging.

In vivo Calcium imaging data analysis

For imaging data analysis, raw image stacks were collected, deconvoluted (if needed), and imported into Image J (NIH) for further analysis. Optical planes from sequential time points were first re-aligned and motion-corrected using a cross-correlation-based image alignment plugin in Image J software to compensate for minor motion change during the acquisition. The contrast was adjusted and selected optical planes or *z*-projections of sequential optical sections were used to obtain final images and to produce time-lapse movies.

Calcium signal amplitudes were expressed as $(F_t-F_0)/F_0$ as a function of time; ratio of fluorescence difference (F_t-F_0) to basal value (F_0). The average fluorescence intensity in the baseline period was taken as F_0, measured as the average pixel intensity during the first 2–6 frames of each imaging experiment. The maximum fluorescence intensity, F_t, was measured by calculating the average (peak – background) pixel values in a given ROI, for each image frame recorded during a time interval before and during the stimulation period. The F_t was then Δ to ΔF/F using the formula $\Delta F/F= (F_t-F_0)/F_0$.

All putative responding cells were verified by visual examination using the raw imaging data. First, analyzers visually scored cells to identify press-evoked calcium transients in DRG neurons, by directly observing the aligned image data displayed as a relative fluorescence movie, as well as the putative responding cells' fluorescence time series. Analyzers defined calcium transients as press-evoked if their onsets occurred between the start of press stimulus and the 7 sec after the end of the stimulus (It takes about 6–7 sec to obtain a full single DRG image). For zoomed-in faster scanning, it takes 0.47 sec/frame to image individual ensembles of coupled neurons. Neuronal coupling was defined as two or more neuronal cell bodies located within 1 μm of each other showing increases in GCaMP signals between two imaging frames. The average ΔF/F values for specific ROIs were tested for statistical significance by repeated measures ANOVA, followed by Mann-Whitney statistics. Image J or Fiji (NIH) and LIF (Leica) software were used to analyze Ca^{2+} imaging data using standard functions and a custom macro.

Systemic and local CBX injection and rhodamine injection

CBX (Sigma) was dissolved in saline. Animals received systemic CBX by i.p. injection. CBX (50 μM in saline) was injected into the DRG from a micropipette by pressure. After the

injection the micropipette was left in the tissue for 4–5 min, it was withdrawn. Rhodamine (Life Technologies) was injected from a micropipette into DRG neurons.

Immunohistochemistry

Adult Cx43 WT control littermate and Cx43CKO animals (12–20 weeks old) with different conditions (naïve, 2 days after CFA, 7 days after nerve injury) were deeply anesthetized with 3% isoflurane and transcardially perfused with 50 ml 0.1 M cold phosphate buffer (PBS) followed by 50 ml PBS containing 4%paraformaldehyde (PFA) (pH=7.4; 4°C). DRGs and lumbar enlargement of the spinal cor d were dissected from the perfused mice, postfixed in 4% PFA at 4°C overnight, cryoprotected in 30% sucrose in PBS at 4°C overnight, and frozen in cryo-embedding media (OCT) at −80°C u sing dry ice. Tissues were transversely sectioned (20 μm) with a cryostat. The sections collected on slides were dried at 37°C for 20 min, then washed with PBS containing 0.2% Triton X-100 (PBT) and blocked with 10% goat or donkey serum in PBT for 1 hr. All sections were simultaneously incubated overnight with primary antibodies diluted in blocking solution at 4°C. Primary antibodies were: rabbit anti-Cx43 (C6219; Sigma; 1:3000), mouse anti-GFAP (Glial Fibrillary Acidic Protein) (CN, MAB360; Millipore; 1:700), rat anti-CGRP (CN, 1720-9007; AbD Serotec; 1:1000), Fluorescein labeled GSL I-isolectin B_4 (CN, FL-1201; Vector Laboratories; 1:1000). After incubation with primary antibody, sections were washed with PBT and then incubated for 2 hrs at room temperature in solutions containing species-specific secondary antibodies conjugated to Alexa 488 or 568 (Molecular Probes). The secondary antibodies were diluted 1:1000 in blocking solution. Following washes with PBS, the stained sections were mounted and coverslipped with Vectashield (Vector Laboratories). The sections were examined and immunostaining images were obtained with a Zeiss 700 scanning confocal microscope.

Dil labeling and imaging

To determine how well the *in vivo* imaging represents the whole population of the DRG neurons, the retrograde nerve tracer Dil (Life Technologies, 0.1% in methanol) was injected into the hindpaws and observed in neuronal cell bodies in the DRG.

DRG cultures

C57BL/6 mice of either sex (2–3 months old; Charles River or Jackson Laboratories, Boston, MA or Bar Harbor, ME, USA) were anesthetized with isoflurane (Abbott Laboratories, IL, USA) and euthanized by decapitation. The DRG were removed as described (Huang et al., 2005) and transferred into cold DPBS (Dulbecco's Phosphate-Buffered Saline, pH 7.4; Mediatech Cellgro, Herndon, VA, USA). Next, they were cleaned from connective tissue and transferred to 1.5 ml vials containing DPBS and collagenase (1 mg/ml, Type 1A; Sigma, St. Louis, MO, USA). The vial was then placed on a tilting stage (with a rate of 50 min^{-1}) for 45 min at 37ºC. After this digestion period the collagenase solution was substituted by fresh DPBS; the ganglia were then triturated by repeated pipetting until tissue dissociation, spun down (1,000 RPM for 5 min), re-suspended and placed in glass-bottomed MatTek dishes (MatTek, Ashland, MA, USA) in Dulbecco's Modified Eagle Medium (DMEM, GIBCO, Invitrogen, Grand Island, NY, USA) supplemented with 10% fetal bovine serum (GIBCO) and 1% Penicillin-Streptomycin (Mediatech Cellgro) and transferred to a humidified 5% CO_2 incubator at 37ºC. Cultures

were generally used at 3–18 hours (for acute culture) or 1–2 days after their preparation when the cultures typically consisted of neurons closely apposed by SGCs, whose identity could be confirmed by their positive immunoreactivity for the marker glutamine synthetase, shape and size and absence of inward currents upon depolarization. Viability of neurons in the cultures was confirmed by their ability to fire action potentials and inducibility of inward currents.

Electrophysiology

Neuron-SGC and neuron-neuron pairs were used for dual whole cell patch clamp recordings performed at room temperature on cells bathed in solution containing (mM): 140 NaCl, 2 $CsCl_2$, 1 $MgCl_2$, 5 HEPES, 2 KCl, 5 Glucose, 2 Sodium pyruvate and 1 $BaCl_2$. Patch pipettes (4–6 MOhms) were filled with solution containing (mM): 130 CsCl (voltage clamp) or 130 KCl (current clamp), 10 EGTA, 10 HEPES, 2 $CaCl_2$ and connected to an Axopatch 1D amplifier (Molecular Devices). Data were acquired with Clampex 6.0 or 8.2 software, digitized using an Axon Instruments Digitizer; and analyzed with Clampfit 9.0 or later software (Molecular Devices). Cells were generally held at −60 mV unless otherwise indicated. Junctional conductance (gj) was calculated as the current recorded in one cell in response to voltage ramps or steps applied to the other cell of the pair (gj=i2/-v1) (del Corsso et al., 2006).

Dye coupling in intact ganglia

After their removal from the animals, DRG were attached to a Sylgard (Dow, Corning, NY)-covered dish filled with cold Krebs solution. The connective tissue capsule around the ganglia was removed by fine dissection. No enzymes were used. The dishes were placed on the stage of an upright microscope (Zeiss, Jena, Germany), equipped with fluorescent illumination and a digital camera. The experiments were started about 30 min after removal. The dish was superfused with Krebs solution, which contained (in mmol/l): 118 NaCl, 4.7 KCl, 14.4 $NaHCO_3$, 1.2 $MgSO_4$, 1.2 NaH_2PO_4, 2.5 $CaCl_2$ and 11.5 glucose; pH 7.3. This solution was bubbled with a mixture of 95% O_2/5% CO_2. Individual cells in DRG were injected with the fluorescent dye Lucifer yellow (LY; Sigma), 3% in 0.5 mol/l LiCl solution from sharp glass microelectrodes, connected to an electrometer (Neuro Data Instruments Corp., New York, NY, USA)(Huang et al., 2005). The dye was passed by hyperpolarizing current pulses, 100 ms in duration; 0.5–1 nA in amplitude at 5 Hz for about 2 min. The injections were made under visual inspection to allow cell identification. At the end of the injection of each cell, we counted the number of cells that were labeled as a result of dye passage from the injected cell (dye-coupled cells). After the experiments the DRG were fixed for 20 hrs at 4°C in 4% PFA in PBS (pH 7.4), washed with PBS and mounted in Gel/mount (Biomeda, Foster, CA, USA). The LY-labeled cells were imaged with a confocal microscope (Biorad).

Analysis

Group data were expressed as mean ± standard error of the mean (S.E.M.). Unless otherwise noted two-tailed unpaired Student's *t* test and/or Mann-Whitney statistical test were used to determine significance in statistical comparisons, and differences were considered significant at $p < 0.05$. Animal behavior data were analyzed with two-way ANOVA test.

Supplementary Material

Refer to Web version on PubMed Central for supplementary material.

Acknowledgments

We thank members of the Dong laboratories for helpful comments and discussion. We also thank JHU pain research imaging core for its assistance. This work was supported by National Institutes of Health Grants (R01DE022750 and R01GM087369 to X.D), Johns Hopkins University Brain Science Institute grant, and HHMI. M.H. was supported by ISF (508/13) and BSF (201144).

References

Amir R, Devor M. Chemically mediated cross-excitation in rat dorsal root ganglia. J Neurosci. 1996; 16:4733–4741. [PubMed: 8764660]

Basbaum AI, Bautista DM, Scherrer G, Julius D. Cellular and molecular mechanisms of pain. Cell. 2009; 139:267–284. [PubMed: 19837031]

Basbaum AI, Woolf CJ. Pain. Curr Biol. 1999; 9:R429–431. [PubMed: 10375535]

Belzer V, Shraer N, Hanani M. Phenotypic changes in satellite glial cells in cultured trigeminal ganglia. Neuron Glia Biol. 2010; 6:237–243. [PubMed: 22032231]

Blum E, Procacci P, Conte V, Hanani M. Systemic inflammation alters satellite glial cell function and structure. A possible contribution to pain. Neuroscience. 2014; 274:209–217. [PubMed: 24875177]

Damodaram S, Thalakoti S, Freeman SE, Garrett FG, Durham PL. Tonabersat inhibits trigeminal ganglion neuronal-satellite glial cell signaling. Headache. 2009; 49:5–20. [PubMed: 19125874]

del Corsso C, Srinivas M, Urban-Maldonado M, Moreno AP, Fort AG, Fishman GI, Spray DC. Transfection of mammalian cells with connexins and measurement of voltage sensitivity of their gap junctions. Nat Protoc. 2006; 1:1799–1809. [PubMed: 17487162]

Devor M, Wall PD. Cross-excitation in dorsal root ganglia of nerve-injured and intact rats. J Neurophysiol. 1990; 64:1733–1746. [PubMed: 2074461]

Doerflinger NH, Macklin WB, Popko B. Inducible site-specific recombination in myelinating cells. Genesis. 2003; 35:63–72. [PubMed: 12481300]

Dublin P, Hanani M. Satellite glial cells in sensory ganglia: their possible contribution to inflammatory pain. Brain Behav Immun. 2007; 21:592–598. [PubMed: 17222529]

Garrett FG, Durham PL. Differential expression of connexins in trigeminal ganglion neurons and satellite glial cells in response to chronic or acute joint inflammation. Neuron Glia Biol. 2008; 4:295–306. [PubMed: 19674505]

Hanani M. Satellite glial cells in sensory ganglia: from form to function. Brain research Brain research reviews. 2005; 48:457–476. [PubMed: 15914252]

Hanani M. Intercellular communication in sensory ganglia by purinergic receptors and gap junctions: implications for chronic pain. Brain research. 2012; 1487:183–191. [PubMed: 22771859]

Huang LY, Gu Y, Chen Y. Communication between neuronal somata and satellite glial cells in sensory ganglia. Glia. 2013; 61:1571–1581. [PubMed: 23918214]

Huang TY, Belzer V, Hanani M. Gap junctions in dorsal root ganglia: possible contribution to visceral pain. European Journal of Pain. 2010; 14:49 e41–11. [PubMed: 19345595]

Huang TY, Cherkas PS, Rosenthal DW, Hanani M. Dye coupling among satellite glial cells in mammalian dorsal root ganglia. Brain Res. 2005; 1036:42–49. [PubMed: 15725400]

Kim YS, Chu Y, Han L, Li M, Li Z, Lavinka PC, Sun S, Tang Z, Park K, Caterina MJ, et al. Central terminal sensitization of TRPV1 by descending serotonergic facilitation modulates chronic pain. Neuron. 2014; 81:873–887. [PubMed: 24462040]

Li L, Rutlin M, Abraira VE, Cassidy C, Kus L, Gong S, Jankowski MP, Luo W, Heintz N, Koerber HR, et al. The functional organization of cutaneous low-threshold mechanosensory neurons. Cell. 2011; 147:1615–1627. [PubMed: 22196735]

Liu Y, Ma Q. Generation of somatic sensory neuron diversity and implications on sensory coding. Curr Opin Neurobiol. 2011; 21:52–60. [PubMed: 20888752]

Ma C, Donnelly DF, LaMotte RH. In vivo visualization and functional characterization of primary somatic neurons. Journal of neuroscience methods. 2010; 191:60–65. [PubMed: 20558205]

Ohara PT, Vit JP, Bhargava A, Jasmin L. Evidence for a role of connexin 43 in trigeminal pain using RNA interference in vivo. J Neurophysiol. 2008; 100:3064–3073. [PubMed: 18715894]

Pannese E. The structure of the perineuronal sheath of satellite glial cells (SGCs) in sensory ganglia. Neuron Glia Biol. 2010; 6:3–10. [PubMed: 20604977]

Rozanski GM, Nath AR, Adams ME, Stanley EF. Low voltage-activated calcium channels gate transmitter release at the dorsal root ganglion sandwich synapse. J Physiol. 2013; 591:5575–5583. [PubMed: 24000176]

Scemes E, Giaume C. Astrocyte calcium waves: what they are and what they do. Glia. 2006; 54:716–725. [PubMed: 17006900]

Schmalbruch H. The number of neurons in dorsal root ganglia L4–L6 of the rat. Anat Rec. 1987; 219:315–322. [PubMed: 3322108]

Sorensen B, Tandrup T, Koltzenburg M, Jakobsen J. No further loss of dorsal root ganglion cells after axotomy in p75 neurotrophin receptor knockout mice. The Journal of comparative neurology. 2003; 459:242–250. [PubMed: 12655507]

Suadicani SO, Cherkas PS, Zuckerman J, Smith DN, Spray DC, Hanani M. Bidirectional calcium signaling between satellite glial cells and neurons in cultured mouse trigeminal ganglia. Neuron Glia Biol. 2010; 6:43–51. [PubMed: 19891813]

Thalakoti S, Patil VV, Damodaram S, Vause CV, Langford LE, Freeman SE, Durham PL. Neuron-glia signaling in trigeminal ganglion: implications for migraine pathology. Headache. 2007; 47:1008–1023. discussion 1024–1005. [PubMed: 17635592]

Zhang H, Mei X, Zhang P, Ma C, White FA, Donnelly DF, Lamotte RH. Altered functional properties of satellite glial cells in compressed spinal ganglia. Glia. 2009; 57:1588–1599. [PubMed: 19330845]

Zuriel E, Devor M. Dye coupling does not explain functional crosstalk within dorsal root ganglia. J Peripher Nerv Syst. 2001; 6:227–231. [PubMed: 11800046]

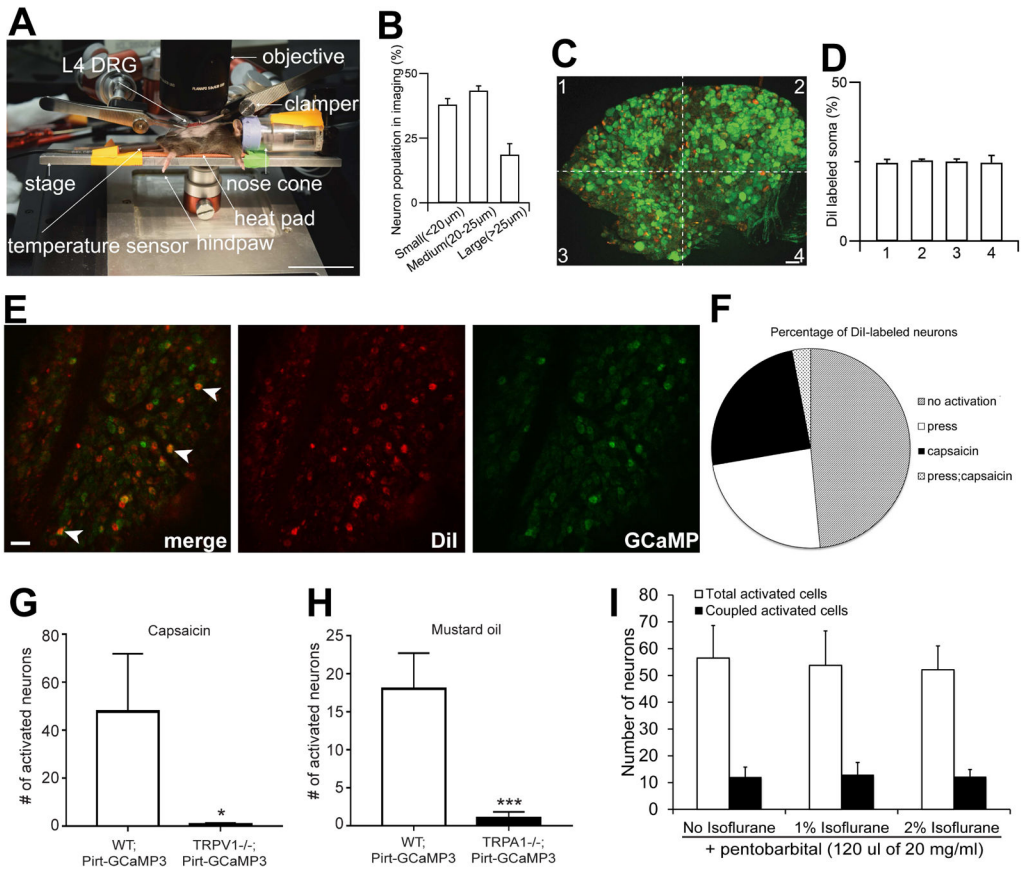

Figure 1. Development of in vivo DRG imaging technique

(**A**) Imaging stage and animal position of *In vivo* intact whole L4 DRG under the microscope. After *in vivo* DRG surgery, the skin is retracted to expose the DRG and the animal rests on a stage attached to two spinal vertebrae clampers on the rostral (L3) and caudal (S1) area. L4 DRG on the right side is exposed and the surface of the DRG is imaged through 5X (NA 0.5) macro dry objective using Leica LSI confocal microscope with 488 green and 568 red diode lasers. One to 2% gas isoflurane is delivered to an animal through a nose cone. A temperature sensor is sensing the animal's rectal body temperature and its body temperature is controlled by a heat pad on the stage. Sensory stimulation (mild mechanical press) is applied to hindpaw. (**B**) Size distribution of small, medium, large neurons in *in vivo* calcium imaging of whole L4 DRG of primary sensory neurons. Quantification of cell sizes was performed after imaging of whole L4 DRG neurons from Pirt-GCaMP3 mice (n=12). (**C**) Distribution of hindpaw projected neurons at L4 DRG level. A hindpaw of Pirt-GCaMP3 mice was Dil injected and imaged several days later (A). Green signal is GCaMP3 protein and Red color is Dil-labeled DRG neurons in L4 DRG (n=7). Scale bars: 40 μm. (**D**) Hindpaw projected neurons are evenly located and distributed on the L4 DRG ganglia. (**E**) Determine the proportion of hindpaw innervating neurons being activated by stimuli applied to the receptive field. A hindpaw of naïve Pirt-GCaMP3 mice was Dil (10μl of 1mg/mL, s.c. plantar surface) injected and imaged 7 days later. GCaMP3 signals were evoked by either pressing the hindpaw (300g) or capsaicin injection (10 μl of 3.3 mM in 0.9% saline, s.c. plantar surface) into the hindpaw (not shown). Arrowheads

indicate Dil labeled neurons being activated by pressing the hindpaw. Scale bars: 40 μm. (**F**) Percentage of of DiI-labeled neurons activated by press (26.4%), capsaicin injection (27.6%), or both (3.4%). n=3. (**G**,**H**) Activation of L4 DRG neurons in response to capsaicin (G, 10 μl of 3.3 mM) or mustard oil (H, 10 μl of 40 mM) was determined by in vivo DRG imaging using Pirt-GCaMP3 in wild-type (WT;Pirt-GCaMP3; n=4) or Pirt-GCaMP3 in TRPV1 knockout (TRPV1−/−;Pirt-GCaMP3; n=3) or TRPA1 knockout (TRPA1−/−;Pirt-GCaMP3; n=4) mice. * $p<0.05$, *** $p<0.005$. unpaired student t-test. (**I**) Determine the effects of different anesthetic reagents on DRG imaging. CFA-treated Pirt-GCaMP3 mice were imaged in the presence of pentobarbital (120 μl of 20 mg/ml, i.p.) with no, 1%, or 2% of isoflurane (n=4). L4 DRG neurons were activated by 300 g press on the hindpaws. The data are presented as mean ± SEM.

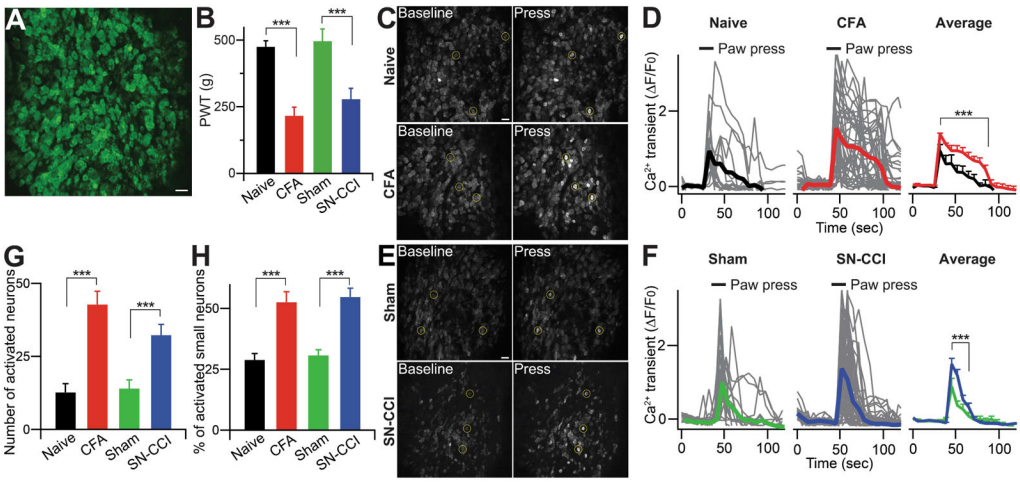

Figure 2. *In vivo* calcium imaging in whole L4 DRG of primary sensory neurons

(**A**) Representative *In vivo* DRG calcium imaging using *Pirt-GCaMP3. In vivo* whole L4 DRG neurons were activated by 100 mM KCl. Scale bar: 50 μm. (**B**) Paw withdrawal threshold (PWT) was tested at the hindpaw of naïve, CFA, sham, SN-CCI animals with rodent pincher analgesia meter. The data are expressed as a PWT value and presented as mean ± SEM. CFA, complete Freund's Adjuvant; SN-CCI, sciatic nerve chronic constriction injury. (**C** and **E**) Representative *in vivo* DRG calcium images showing in $[Ca^{2+}]_{in}$ increase in DRG neurons and (**A** and **F**) Time course of the amplitude of the calcium transient that was evoked by mild mechanical press (using rodent pincher, 300 g) at the hindpaw from naïve, CFA, sham, SN-CCI animals. Some examples of activated DRG neurons are circled. Each trace is a response from a single DRG neuron. All data for calcium transient are expressed as the percentage of baseline calcium transient ($\Delta F/F_0$) and are presented as mean ± SEM. Black bars indicate when stimuli were applied. Scale bar: 50 μm. (**G**) Number of neurons activated by mild mechanical press to naïve, CFA, sham, SN-CCI animals. (**H**) Percentage change of small diameter neurons (< 20 μm) activated by mild mechanical press to naïve, CFA, sham, SN-CCI animals. The data are presented as mean ± SEM. ***, $p<0.001$.

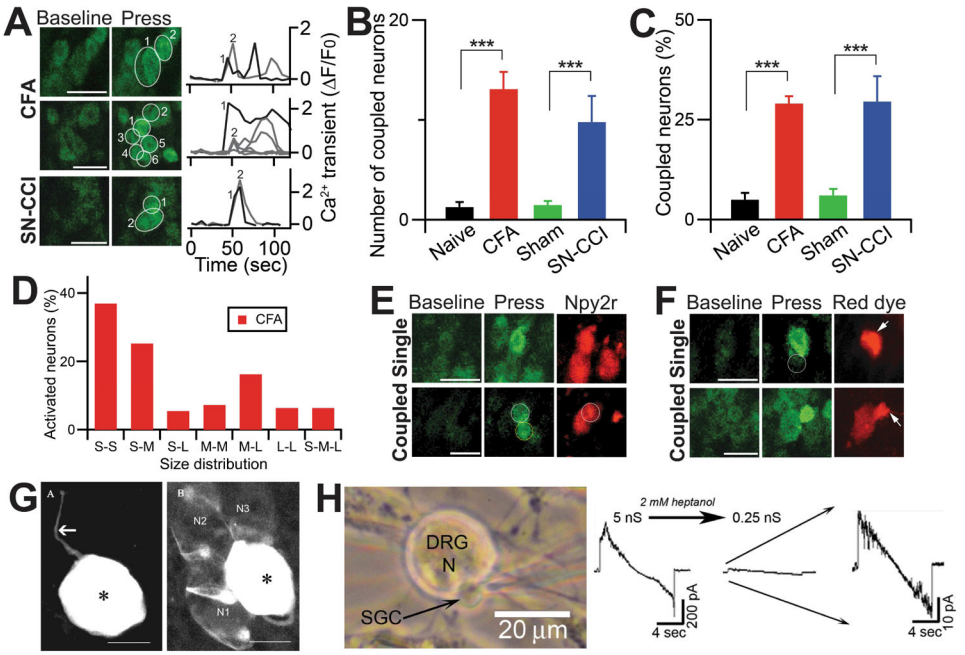

Figure 3. Coupled activation of adjacent DRG neurons in *in vivo* DRG calcium imaging

(**A**) Representative images of coupled events in *in vivo* calcium imaging of Whole L4 DRG neurons. Left panels, adjacent DRG neurons tend to activate together when stimuli (mild mechanical press; 300g) were applied to the hindpaws of CFA and SN-CCI animals. Right Panels, Time course of the amplitude of the calcium transient that was evoked by mild press at the hindpaw from CFA and SN-CCI animals. Each trace is a response from a single DRG neuron and number indicates the order of DRG neuron activated by press stimuli. All data for calcium transient are expressed as the percentage of baseline calcium transient ($\Delta F/F_0$). Scale bar: 50 μm. (**B**) Number of coupled neurons activated by mild press to naïve, CFA, sham, and SN-CCI animals. (**C**) Quantification of coupled neurons, normalized by total number of neurons activated by mild press to naïve, CFA, sham, and SN-CCI animals. ***, $p<0.001$. (**D**) Percentage of coupled neuron according to the size of each member of the pair. S, small-diameter DRG neurons (<20 μm); M, medium (20–25 μm); L, large (>25 μm). (**E**) Representative *in vivo* images of neurons labeled for NPY2r-tdTomato, a marker for large-diameter, rapid adapting, low threshold mechanoreceptor (Aβ-LTMR), activated singly in naïve and coupled in CFA animals. Scale bar: 50 μm. (**F**) Representative *in vivo* images of neurons labeled with rhodamine. Dye transfer was observed only in CFA animals. Circle indicates an adjacent DRG neuron. Arrows indicate where rhodamine was injected into a DRG neuron. Scale bar: 50 μm. (**G**) Direct evidence for neuron-SGC coupling by gap junctions. Confocal images obtained with the dye transfer method using intracellular injection of Lucifer yellow (LY). (Left) An uncoupled neuron with its axon (arrow) in a ganglion from a 3 months old mouse. (Right) A dye-injected neuron (asterisk) was coupled to SGCs around three neighboring neurons (N1–N3) in a ganglion from a 12 months old mouse. SGCs around the labeled neuron are probably labeled, but they cannot be visualized because of masking by the bright staining of the neuron. Asterisks mark the dye-injected cells. Scale bars, 20 μm. (**H**) Dual patch clamp recordings from neuron-SGC pairs. The cells were clamped at 0 mV, a voltage ramp (from −100 to +100mV) was applied to the neuron,

and current was recorded in an adjacent SGC. Left panel, the configuration of neuron and SGCs is shown. Right panel, the addition of the gap junction blocker heptanol (2 mM) reduced gap junction-mediated electrical conductance between the neuron and SGC, which was high (5 nS) in the control but was reduced to 0.25 nS, reduction by a factor of 20. Scale bar: 20 μm.

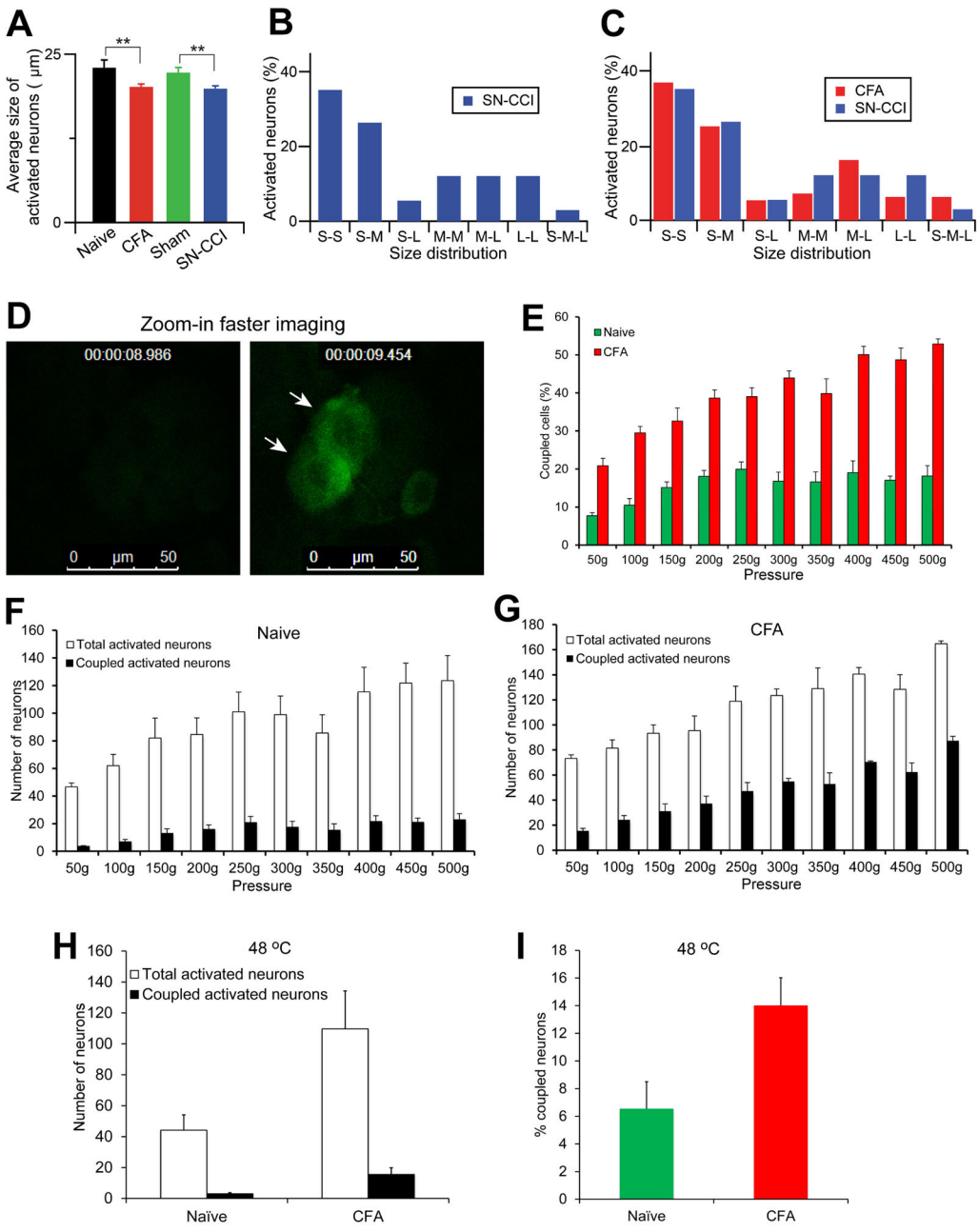

Figure 4. Characterization of coupled activated neurons in the DRG

(**A**) Average size of activated neurons in *in vivo* DRG calcium imaging from Pirt-GCaMP3 mice. Total average size of activated neurons was measured with mild mechanical press stimuli from different conditions (naïve, CFA, sham, and SN-CCI) Pirt-GCaMP3 mice (n=10). (**B**,**C**) Size distribution of coupled activated neurons. Percentage and distribution of coupled activation DRG neurons are determined according to the cell size of each member of the pair. S, small-diameter DRG neurons (<20 um); M, medium (20–25 um); L, large (>25 um). (**D**) Examining simultaneous activation by zoomed-in faster imaging. L4 DRG in CFA treated Pirt-GCaMP6 mice (n=3) were imaged first at ~6 sec/frame to identify coupled

activated neurons in the entire exposed DRG areas. Then imaging was zoomed in on one ensemble of coupled activated neurons with much higher frequency (0.47 sec/frame; time point was indicated at the top of the images). Two arrows indicate two simultaneously activated neurons. (**E**–**G**) Dose responses of L4 DRG neuron activation in response to mechanical press (from mild 50 g to noxious 500 g) using naïve or CFA treated Pirt-GCaMP6 mice (n=3 per group). The percentage of coupled activated neurons in (E) was calculated from the number of coupled activated neurons divided by the number of total activated neurons (F for naïve mice, G for CFA-treated mice). (**H**,**I**) Examining neuronal coupling in response to noxious heat (48 °C) in naï ve and CFA-treated Pirt-GCaMP3 mice. There are significant increases in the numbers of total activated neurons and coupled activated neurons (H) and the percentage of coupled activated neurons in CFA-treated mice compared to naïve mice (n=3; $p<0.05$). The data are presented as mean ± SEM.

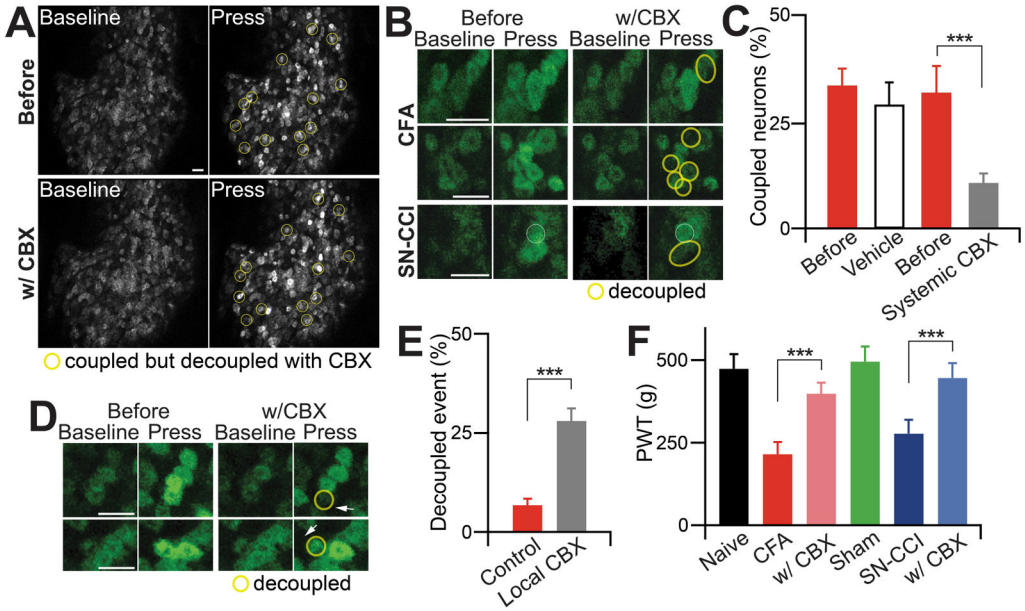

Figure 5. Coupling event and pain hypersensitivity are significantly attenuated by the gap junction blocker carbenoxolone (CBX)

(**A**) Representative images of coupled and decoupled events before and approximately 1 hr after systemic gap junction blocker, CBX injection (100 mg/kg, i.p.) in *in vivo* calcium imaging of whole L4 DRG neurons. Yellow circles indicate coupled events in which adjacent DRG neurons tend to activate together, and these coupled events decoupled by systemic CBX. Scale bar: 50 μm. (**B**) Example images of coupled and decoupled events by systemic application of CBX. Yellow circles indicate the coupled DRG neurons decoupled by systemic CBX. Scale bar: 50 μm. (**C**) Percentage change of coupled DRG neurons out of total activated DRG neurons by vehicle or CBX. (**D**) Decoupled images of coupled events by local CBX injection using glass pipette electrode into DRG tissue. Yellow circles indicate decoupled DRG neurons. Arrows indicate where CBX was injected into the DRG tissue. Scale bar: 50 μm. (**E**) Quantification of decoupled events in control coupled events and coupled events after local CBX injection into DRG tissue. (**F**) Paw withdrawal threshold (PWT) was tested at the hindpaw of naïve, CFA, CFA with CBX, sham, SN-CCI, and SN-CCI with CBX animals by rodent pincher. The data are presented as mean ± SEM. ***, $p<0.001$.

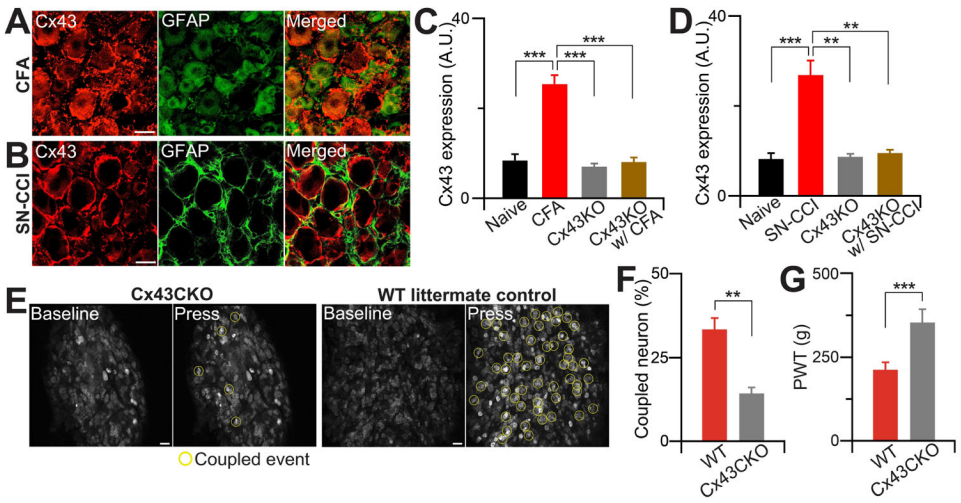

Figure 6. Gap junction protein, Cx43 promotes coupling event and contributes to pain

(**A**) Representative confocal images of Cx43 and GFAP staining from DRG of WT littermate control animals after inflammation. DRG from mice 2 days after CFA injection were stained with anti-GFAP (for SGCs; green) and/or anti-Cx43 (red) antibodies. Scale bar: 20 μm. (**B**) Representative confocal Cx43 and GFAP staining images from DRG of WT littermate control animals after nerve injury. DRG slices from mice 7 days after nerve injury were stained with anti-GFAP (green) and/or anti-Cx43 (red) antibodies. Scale bar: 20 μm. (**C, D**) Percentage change of Cx43 levels in DRG from naïve and CFA (**C**) or SN-CCI (**D**) treated WT animals and also from conditional Cx43CKO animals. Data are expressed as the mean density. Cx43 level from WT DRG (n=10, 8.44±1.38 arbitrary unit (a.u.)), CFA DRG (n=10, 25.42± 1.99), CCI DRG (n=8, 26.83±3.30); Cx43CKO DRG (n=10, 7.04± 0.68). (**E**) Representative *in vivo* confocal images of whole L4 DRG neurons from Cx43CKO and WT littermate control animals after CFA. Yellow circles indicate coupled event. (**F**) Percentage change of coupled DRG neurons from Cx43CKO and WT littermate control animals (i.e. Cx43 flox allele without PLP-Cre mice). (**G**) Paw withdrawal threshold (PWT) was tested in Cx43CKO and WT littermate control animals with rodent pincher. The data are expressed as PWT values and presented as mean ± SEM. **, p<0.01; ***, p<0.001.